International Journal of Low-Carbon Technologies, 2024, **19**, 1660–1673
https://doi.org/10.1093/ijlct/ctae115
Original Article

Thermal comfort inside a gable-roofed metallic shed in a higher educational institution: a case study and detailed analysis

Abubakkar Abdul Jaffar[1], Selvakumar Pandiaraj[2], Kumaresan Govindasamy[3], Kamal Sharma[4], Suresh Muthusamy[5], Mohammad Irfanul Haque Siddiqui[6], Erdem Cuce[7,8], Mohd. Asif Shah[9,10,11]*

[1]Leadership Boulevard Private Limited, Tiruchirappalli-620011, Tamil Nadu, India
[2]Department of Mechanical Engineering, Kongu Engineering College (Autonomous), Perundurai, Erode-638060, Tamil Nadu, India
[3]Department of Mechanical Engineering, Bannari Amman Institute of Technology (Autonomous), Sathyamangalam, Erode-638401, Tamil Nadu, India
[4]Department of Mechanical Engineering, GLA University, Mathura-281406, India
[5]Department of Electrical and Electronics Engineering, Kongu Engineering College (Autonomous), Perundurai, Erode-638060, Tamil Nadu, India
[6]Department of Mechanical Engineering, King Saud University Riyadh 11495, Saudi Arabia
[7]Department of Mechanical Engineering, Faculty of Engineering and Architecture, Recep Tayyip Erdogan University, Zihni Derin Campus, 53100 Rize, Turkey
[8]School of Engineering and the Built Environment, Department of Mechanical Engineering, Birmingham City University, B4 7XG, Birmingham, UK
[9]Department of Economics, Kebri Debar University, Kebri Debar, Ethiopia
[10]Division of Research and Development, Lovely Professional University, Phagwara, Punjab, 144001, India
[11]Centre of Research Impact and Outcome, Chitkara University Institute of Engineering and Technology, Chitkara University, Rajpura-140401, Punjab, India

*Corresponding author. Department of Economics, Kebri Debar University, Kebri Debar, Ethiopia. E-mail: drmohdasifshah@kdu.edu.et

Abstract

Central workshop is an integral part of any higher education institution, and it will be generally operated in a gable-roofed metallic shed. The users of the building are affected physiologically and psychologically due to the thermal discomfort conditions caused by improper ventilation. It is necessary to study the cause for discomfort and propose cost and effective methods to mitigate the problem. In this work, the thermal comfort inside a gable-roofed workshop was analyzed, and it was found that the discomfort was predominant from 2 PM to 5 PM. It was predicted that the conduction heat transfer could be reduced upto 55% with the help of passive cooling technique carried out using aluminium bubble wrap. During the life cycle cost study, the aluminium bubble wrap technique was found to be more economical over high-volume low-speed fan. The computer simulation aided in the prediction of overall heat transfer coefficient and conduction heat transfer through wall. The results from numerical study deviated by less than 0.1% when compared with that from the theoretical model.

Keywords: gable-roofed shed; thermal discomfort; passive cooling techniques; numerical analysis; life cycle cost

1 Introduction

Central workshop is an integral part of any higher education institution, and they generally possess metallic roofing. There will be one or two office rooms and the remaining built-up area will be used for the machineries and its operators. The users of the building are subjected to mental and physical stress due to the thermal discomfort. In large enclosed space, the working condition is improved with the help of large sized high-volume low-speed (HVLS) fan [1]. The options of using passive cooling methods are yet to be studied in metallic sheds. Thermal comfort in general is about a person describing his state of mind about the thermal conditions of the area. It cannot be indicated by a single temperature but can be described by the number of employees complaining of thermal discomfort. Environmental, personal, and work-related factors also influence the degree of comfort [2]. Predicted mean vote, physiological equivalent temperature, standard effective temperature, perceived temperature, and thermal balance are some of the thermal indices used to study the thermal comfort. They can be calculated by the properties of air and radiation. The degree of thermal comfort on productivity was established by many researchers and standards [3]. American Society of Heating, Refrigerating and Air-conditioning Engineers (ASHRAE) Standard55-2010 [4] and ISO7730:2005 [5] are the standard benchmarks for thermal comfort surveys. This type of survey helps in knowing the present condition of the work place. Extreme temperatures can have adverse effects on human mind and body. Figure 1 shows the human body temperature and its corresponding effects [6]. The work space is thermally comfortable if the Predicted Mean Vote

Received 17 December 2023; revised 16 April 2024; accepted 29 June 2024

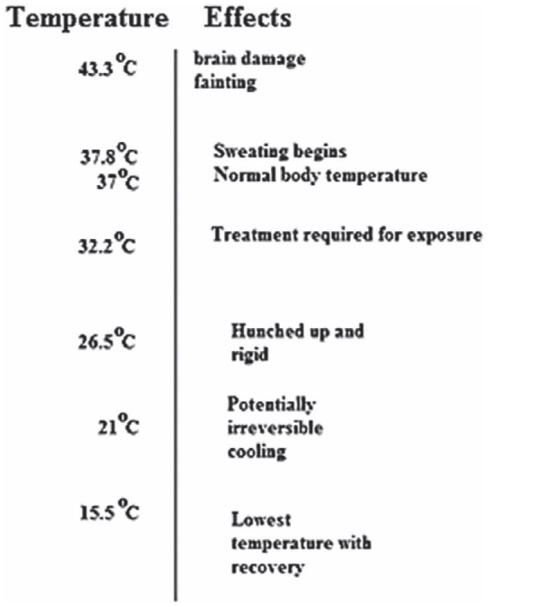

Figure 1. Effects on body at various temperatures.

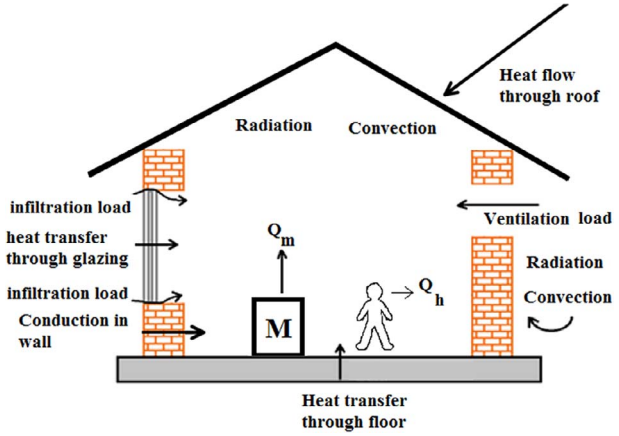

Figure 2. Heat flow in gable roof shed.

(PMV) lies between −0.5 to +0.5, and the predicted percentage of dissatisfied is 10% [7]. Thermal comfort can be ascertained using questionnaire or by measurements of physiological changes. Thermal comfort surveys based on PMV overestimate the thermal sensation of human beings. In a tropical country, every one prefer a cooler than a neutral environment [8].

Passive house, green building, and bioclimatic design are some of the ways to lower the energy consumption in buildings. Heat transfer in buildings is usually not well defined due to the interaction of various physical parameters and underlying assumptions. Design of building envelope [9] with proper considerations being given in the initial phase helps in optimizing the energy demand. To have a comfortable environment inside the building envelope, the building materials are to be chosen with lower thermal conductivity.

The conduction heat transfer mainly occurs through the building walls [10] and is proportional to the temperature difference of the inside and outside walls. Convection occurs due to the bulk motion of air in contact with the surfaces. Radiation heat transfer occurs mainly due to the solar heat gain [11]. The building envelope can be assumed as a barrier separating the interior of the house from external environment. They protect the inside space within a building from undesirable effects of environment [12]. Conduction heat transfer occurs mainly in the opaque surfaces of the building envelope such as walls, roof material, and floor. A simplified heat transfer process in a room with gable roof is shown in Fig. 2.

Thermal resistance method can be used to study the steady state one dimensional heat flow through a wall. The heat flow depends on the resistance and temperature difference. In actual wall, many layers of materials with different thermal conductivity are present. The conventional insulating materials absorb or slow down the heat transfer. The rate in which the absorbed heat transfers through insulation is called as material's R-Value. Studies were conducted to understand the heat gain in a building using energy plus software. It was concluded that the fly ash brick with grey glass window received the lowest heat gain [13]. Compared to the time-dependent model, the steady-state model overestimates the thermal load in an air-conditioned system [14]. The heat transfer through a composite wall was analysed numerically using finite-volume method, and the solutions were obtained with the help of Gauss–Seidel method [15]. Kim *et al*. [16] investigated the energy performance of a building using cold roof and warm roof. Varol *et al*. [17] investigated the effects of natural convection heat transfer in gable roofs and the governing equation in stream wise vorticity function were solved using finite difference method. Rayleigh number, wavelength, and aspect ratio affect the heat transfer in a sloped roof. The increase in temperature of the indoor due to solar radiation may include solar heat transmission, solar heat absorption, and reflection by interior building surfaces. Time lag and decrement factor are the main parameters that have to be considered in the thermal performance of the walls. Many methods were developed in the past to give passive cooling and heating effect inside the building envelope. Conical roof transfers 30% lower heat than that of flat roof [18]. Buildings with Fresnel lens integrated into it can minimize the energy consumption for heating appliances. The solar energy falls on a conducting material can also be transferred to a phase change material [19]. Radiative cooling is done using paints, coatings, phase change materials, rare earth elements, volcanic soil, and deposits. The emissivity and absorptivity play a significant role in the radiative cooling process [20]. A decrease in temperature of 2.6°C was obtained using cool roof. This technology when used with a cool facade painting reduced the temperature by 3.1°C [21]. Plants such as *Amaranthus hybridus* and *Brassica juncea* can be used in hot humid tropical climates for temperature reduction in the house [22].Porous material developed using rice husk also provides cooling effect. This is due to the capillary action of water in a hollow cylindrical shaped body [23]. Solar chimney removes the hot air and brings the indoor air to a lower temperature. Analytical model to predict the performance of solar chimney were also developed. Hot air from outside can be trapped in a wind tower, which then gets cooled due to the heat loss from the air to water [24]. Solar photo voltaic (PV) in roofs help to reduce the amount of radiation entering the building envelope from the roof. Also it generates power which can be used to run the systems inside the building. Selvakumar *et al*. [25] studied the solar heat gain variation in building with rooftop photovoltaic plant. Thermal imaging showed that the temperature on a surface below the PV panel was 2.5°C lesser than the exposed roof. The adequate amount

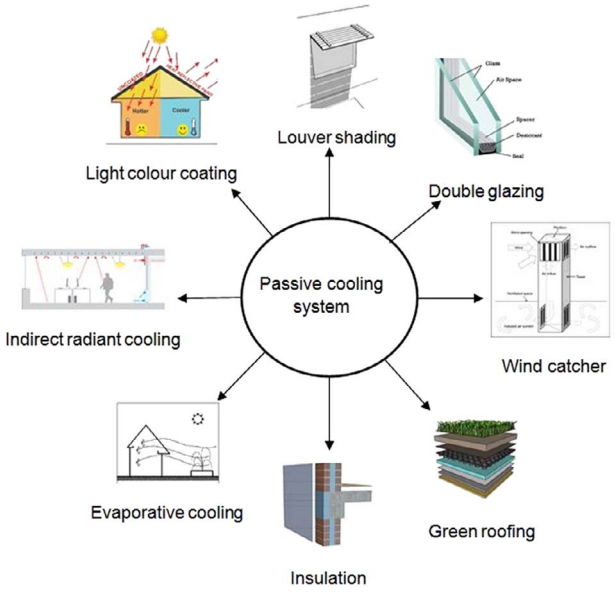

Figure 3. Passive cooling in buildings.

of airflow in an area can be created by a HVLS fan. Airflow is the volume of air moved by a fan per unit time, usually expressed in cubic feet per minute (CFM). Ventilation is measured in terms of air changes per hour (ACH) [26]. Airflow for ventilation can be calculated by area method, air change method, occupancy method, and heat removal method. Radiant barrier is a highly reflective material which blocks the transfer of radiant heat by reflecting it away from its surface. A radiant barrier insulation system is a layer of reinforced aluminium foil facing airspace inside a building. Susan Abed Hassan studied on ways to reduce energy consumption by insulating building envelope according to cooling degree days [27]. The study indicated that there were variations in cooling degree days for major Iraqi cities, and there was an effect of building envelope insulation on cooling energy loss, with wall insulation reducing consumption energy by 70–80%. In addition, when compared with the identical building materials without insulation, ceiling insulation decreased energy usage by 65%. Yiyun Zhu and Xianling Wang studied the thermal performance of aluminium foil bubble composites on the underside of the roof in the attic area in the Qinba Mountains [28]. Radiant barrier materials with an emissivity of less than 0.3 and a thermal resistance of not more than 2 m^2 KW^{-1} were recommended based on thermal performance and cost studies. Indirect radiant cooling is the method of net emission of electromagnetic waves from heated region to cooled region and it continues till the temperature of both regions become same [29]. External walls exposed to the direct sun light receives high radiation from sun and gets heated more which is transferred to the interior surface. To reduce this, solar reflective coatings can be applied in the exterior surface of the exposed walls. As a summary of the above discussion, the passive cooling techniques [30] used for improving room ambience were identified and depicted in Fig. 3.

Use of air conditioning system and fans is an active cooling method for room comfort. High volume low speed (HVLS) fans are being used in few automobile industries for providing thermal comfort through active cooling. HVLS fan are being popularly used in mosques [31] and warehouses [32] as a part of green and sustainable approach in building construction sector. HVLS fan comes under active cooling method which consumes considerable high electrical energy. It is also important to study the life cycle cost involved in the chosen technology. Life cycle cost analysis (LCCA) helps to make clear decision by considering the long term profitability and competitiveness [33]. In this article, the factors influencing the thermal comfort were studied initially. For improving the thermal comfort by passive cooling technique, aluminium bubble wrap insulation was adopted for the gable-roofed metallic shed. As this passive method was novel for a gable-roofed metallic shed, the change in thermal comfort due to active method was also studied for getting a fruitful conclusion. The cost and energy required for maintaining a comfortable indoor environment through active and passive techniques were studied in detail. For the case of active method, HVLS fan was considered in this work. The outcome of this study will help in designing a passive green building for laboratory purpose in higher education institutions.

2 Methodology

A shed of dimension 25 m × 31.160 m is considered for investigation. Inside the shed, there are four different working spaces namely, renewable energy laboratory, machining process laboratory, working model laboratory, and faculty cabin. The workshop is surrounded by compound wall on one side, buildings on the other two sides. The thickness of the wall is 250 mm, which includes a 12.5 mm layer of plaster on both sides of the brick. The front portion of the workshop is open for ventilation and air movement. Around 30% of the total area of the font wall is left for ventilation. The workshop is having gable type roof with GI sheet as the roofing element. The dimensions of the workshop are shown in Fig. 4.

During the summer season, the temperature of workspace under the shed increases above 35°C. This causes a lot of thermal discomfort to the persons inside the workshop. This thermal discomfort is further exacerbated due to the absence of ceiling fans in the work area. Fans are available but they are wall mounted which could not provide proper comfort and air circulation to the people inside the workshop. The detailed workflow methodology is shown in Fig. 5.

A survey was conducted among 174 persons involved in work activity inside the shed. Data regarding the occupant perception and satisfaction are obtained with respect to the air temperature, radiant temperature, humidity, air movement, and metabolic rate. The surface and air temperatures are observed for a period of 24 hours during the month of March 2020. The temperatures on the four inner sides of the envelope are named as T_{ni}, T_{wi}, T_{si}, and T_{ei}, respectively. The inner side of the metallic roof temperature is named as T_{5i} on the north side and T_{6i} on the south side of the building. Similar naming convention has been followed for outer surfaces also. The inside, outside, and cabin air temperatures are T_{ai}, T_{ao}, and T_{ac}, respectively. Based on the temperature readings, the amount of heat entering the building envelope is determined. ANSYS has been used to simulate the temperature distribution inside the shed.

2.1 Energy balance in a gable roof shed

The heat energy entering the system is either used to increase the energy content of the air or the energy content of the building envelope. The heat transfer can be found by the knowledge

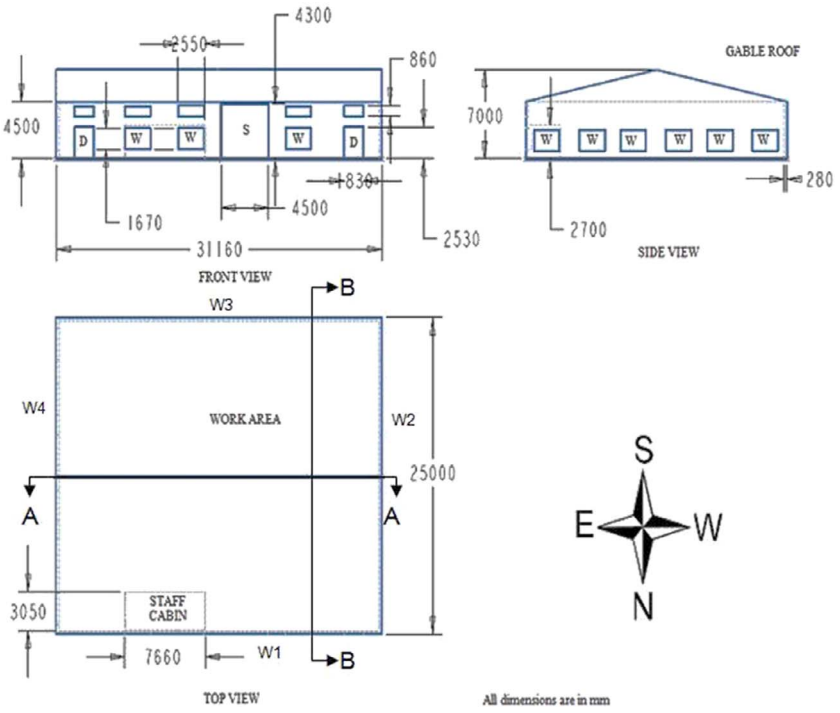

Figure 4. 2-Dimensional views of workshop.

of temperature and material properties. The equation for the indoor air temperature at a particular time can be derived based on frequency domain treatment [34]. $\overline{T}$ is the average temperature, and it is found to be 30.61°C. Heat energy flows from high temperature to low temperature by conduction, convection, and radiation. The energy balance according to the first law of thermodynamics is given by the equation:

$$E_{ia} + E_{ib} + Q = E_{fa} + E_{fb} \tag{1}$$

In Equation 1, E_{ia} is the energy content of air at time t inside the system, E_{ib} is the energy stored in the building envelope at time t, E_{fa} is the energy content of air after a time period Δt, E_{fb} is the energy stored in the building envelope after a time period Δt, and Q is the amount of heat entering the system. Equation 1 is derived by assuming the building envelope as a thermodynamic system and applying the first law of thermodynamics. From the above equation, the total amount of heat entering the building envelope is calculated. The heat transfer through walls happens mainly by conduction which can be calculated as follows.

$$Q = U\,A\Delta T \tag{2}$$

The overall thermal transmittance of the wall is given by 2.13 W/m^{2}K. The heat transfer through the walls, roof, and the floor are calculated individually to estimate the total amount of heat entering the system. This can be done by assuming the wall to be vertical surface, floor to be horizontal surface, and the roof to be inclined surface. The convection heat transfer from the wall is given by Equation (3). The heat transfer coefficient for the walls is taken as 6 W/m^{2}K [35]. The thermal properties of the building materials are mentioned in Table 1.

The wall taken for study is composite system. By applying Fourier law of heat conduction to the three layered wall, the resistance diagram can be drawn as shown in Fig. 6.

The basic heat transfer relations represented from Equations (3) to (9) are referred from [37].

The heat transfer through the wall is given by

$$q = -KA\frac{dT}{dx} \tag{3}$$

By Equation (3), the intermediate temperatures of the composite wall can be calculated by Equations (4) and (5)

$$T_b = T_a - \left(\frac{T_a - T_d}{\Sigma R}\right) R_1 \tag{4}$$

$$T_c = \left(\frac{T_a - T_d}{\Sigma R}\right) R_3 + T_d \tag{5}$$

For determining the temperature at any point in the composite wall is derived below.

Equation (6) is the three-dimensional heat conduction equation.

$$\frac{\partial^2 T}{\partial x^2} + \frac{\partial^2 T}{\partial y^2} + \frac{\partial^2 T}{\partial z^2} + \frac{g}{k} = \frac{1}{\infty}\frac{\partial T}{\partial t} \tag{6}$$

The heat conduction in composite wall is one dimensional occurred by steady-state conduction without any internal heat generation.

The temperature in plaster 1 at x distance from origin is determined by Equation (7)

$$T = \left(\frac{T_b - T_a}{L_1}\right) x + T_a 0 \le x \le L_1 \tag{7}$$

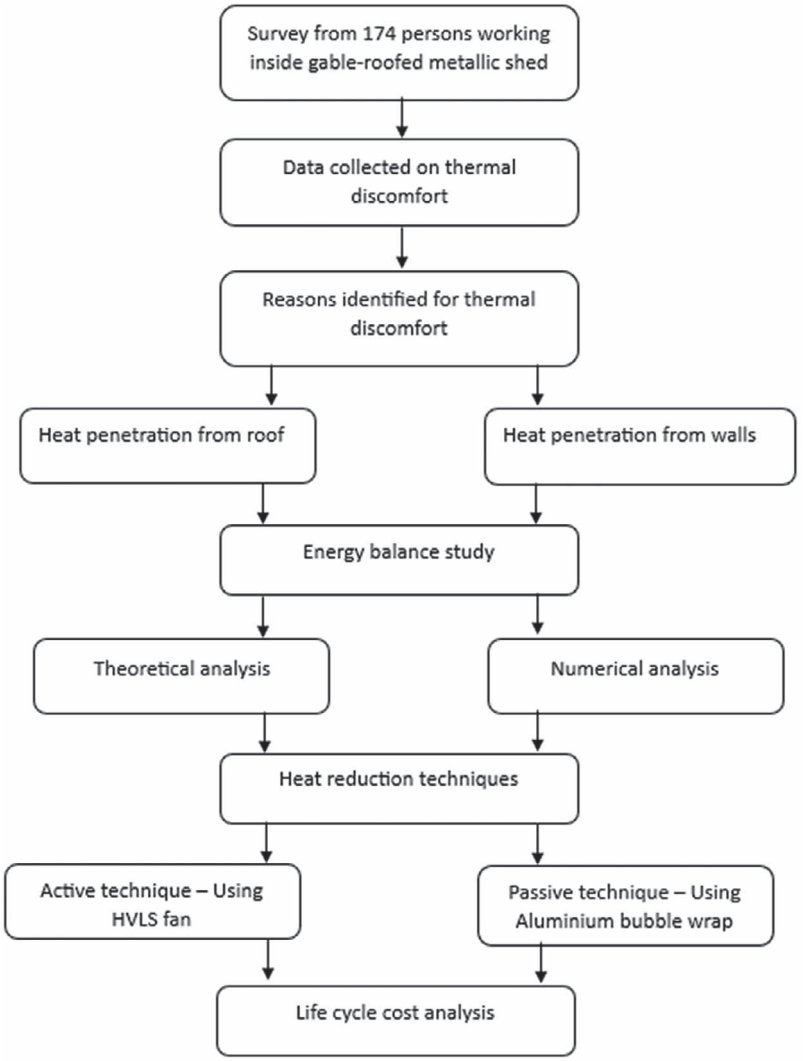

Figure 5. Workflow methodology.

Table 1. Thermal properties of building materials [36].

Property	Brick	Cement plaster	Metallic roofing
Thermal conductivity in W/m K	0.811	0.721	61.06
Density in kg/m^3	1820	1762	7520
Specific heat capacity in J/kg K	880	840	500
Thermal diffusivity in m^2/s	5.06×10^{-7}	4.87×10^{-7}	—

The temperature in brick at x distance from origin is determined by Equation (8)

$$T = \left(\frac{T_c - T_b}{L_2}\right) x + T_b - \frac{(T_c - T_b)}{L_2} x L_1 \qquad (8)$$
$$L_1 \le x \le L_1 + L_2$$

Similarly, temperature in plaster 2 at x distance from origin is determined by Equation (9)

$$T = \left(\frac{T_d - T_c}{L_3}\right) x + T_c - \left(\frac{T_d - T_c}{L_3}\right) (L_1 + L_2) \qquad (9)$$

$$(L_1 + L_2) \le x \le (L_1 + L_2 + L_3)$$

2.2 Simulation

The steady-state thermal analyses of the composite walls are analysed in ANSYS 2020 R1 software. The nature of convection heat transfer in the workshop complex is studied by ANSYS simulation. For simulation in ANSYS fluent, the workshop complex is considered as two 2D surfaces. One 2D surface is obtained along section A–A shown in Fig. 4. This gives a rectangular section. Another 2D surface is obtained by section B–B as in Fig. 4 which gives a triangle on the top of a rectangular section. The generated mesh has 6212 elements and 6421 nodes as shown in the rectangular section. For triangle over the rectangle, 3237 elements and 3444 nodes are created during meshing. The meshed geometry is shown in Fig. 7. The quality of the mesh can be checked using skewness value [38]. Grid independency test was performed on the

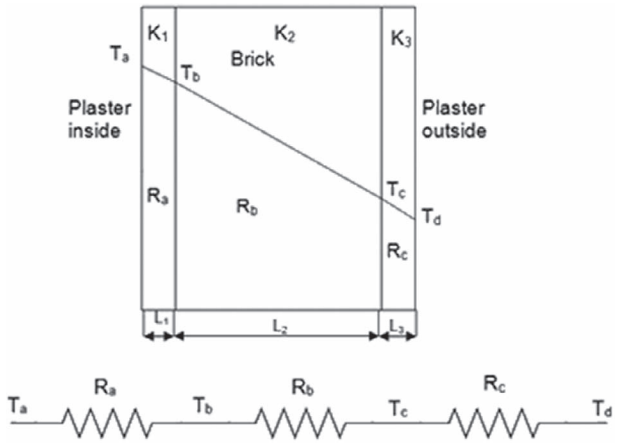

Figure 6. Schematic and resistance diagrams of composite wall.

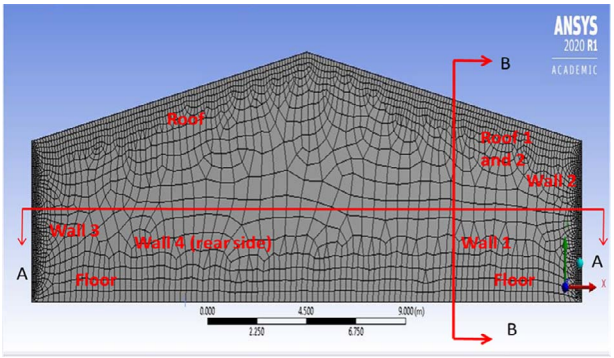

Figure 7. Meshed geometry.

Table 2. Boundary conditions of section A–A.

Surface	Temperature (K)
Floor	312
Roof	325
Wall 4	310.8
Wall 3	311.4

generated mesh and an equiangle skewness value of 0.4 was arrived. The heat from the walls and roof contribute to the increasing room temperature by convection heat transfer.

The temperatures of the walls, floor, and roofs are assigned as boundary conditions for solving the natural convection heat transfer problem, and they are listed in Tables 2 and 3. The purpose of the simulation is to predict the temperature distribution in the walls which will aid in the selection of passive cooling technique for the building.

2.3 Reduction of heat transfer in walls

The study on reduction of heat transfer in walls is depicted in this section. For this study, two thermal models are created. One is conventional composite walls, and another one is insulated wall. The insulating material taken for this study is aluminium bubble wrap of varying thickness. The thermal conductivity of aluminium bubble wrap is considered as 0.038 Wm^{-1} K^{-1} [39]. The inside air temperature is assumed to be 25°C (T_2) for comfort inside the workshop complex. The outside temperature varies from 25°C to 37°C (T_1). Thermal conductivity of air outside and inside is assumed as 23

Table 3. Boundary conditions of section B–B.

Surface	Temperature (K)
Floor	312
Roof 1	324.5
Roof 2	327.8
Wall 1	309.8
Wall 2	311.6

$Wm^{-1}K^{-1}$ and 9 Wm^{-1} K^{-1} [40].Thermal transfer coefficient (U) for the buildings is limited to certain level by considering the climatic condition of the country by their international standards organization. For India, the U value is standardized by Bureau of Indian standards in IS: 3792–1978. Various regions of India are categorized by four temperature and humid zones which are mentioned in Table 4.

The maximum dry bulb temperature and relative humidity figures presented here are based on the conditions prevailing in India during summer season. These data are specifically considered in this study because the thermal discomfort is experienced heavily in summer season under gable-roofed metallic shed.

Based on the bureau of Indian standard IS: 3792-1978, the workshop complex chosen for study comes in the region of hot and humid zone. From Table 5, the U_{max} value is chosen as 2.56 W/m^2K. Further calculations of the thermal transfer coefficient for developed thermal models are calculated and compared with this U_{max} value. For the first thermal model of conventional wall, the thermal transfer coefficient (U) and conductivity heat transfer (Q) are calculated by Equations (10) and (11), respectively. For this study, the area of wall is assumed to be 1 m^2.

$$U = \frac{1}{\Sigma R} \tag{10}$$

$$Q = \frac{T_1 - T_2}{\Sigma R} \tag{11}$$

The thermal model and resistance diagram for the conventional and insulated wall are shown in Figs 8 and 9.

$$\frac{1}{h_1} + \frac{La}{Ka} + \frac{Lb}{Kb} + \frac{Lc}{Kc} + \frac{1}{h_2} = \Sigma R \tag{12}$$

$$\frac{1}{h_1} + \frac{La}{Ka} + \frac{Lb}{Kb} + \frac{Lc}{Kc} + \frac{Ld}{Kd} + \frac{1}{h_2} = \Sigma R \tag{13}$$

By using ΣR of two thermal models in the Equations (10) and (11), the U value and Q value of insulated wall are calculated. The reduction in conduction heat transfer due to the aluminium bubble wrap is analysed in ANSYS steady state thermal model. For this study, a wall of unit area is generated in geometry with three layers for conventional wall and four layers for insulated wall. The thickness of aluminium bubble wrap considered here is 8 mm. Generated geometry is meshed with the element size of 30 mm which generates 67 550 nodes and 12 716 elements. The generated mesh geometry is shown in Fig. 10. Convective film coefficients of air and ambient temperature mentioned in Table 6 are given as boundary conditions of the wall.

Table 4. Temperature and humid zones [41].

Zone	Maximum dry bulb temperature (°C)	Relative humidity
Hot and arid	38	40% or less
Hot and humid	32	Above 40%
Warm and humid	26–32	Above 70%
Cold	Minimum 6 or less	-

Table 5. Thermal performance standards.

Building component	Hot dry and humid zone U_{max} (W/m^{2}K)	Warm humid zone U_{max} (W/m^{2}K)
Roof	2.33	2.33
Exposed wall	2.56	2.91

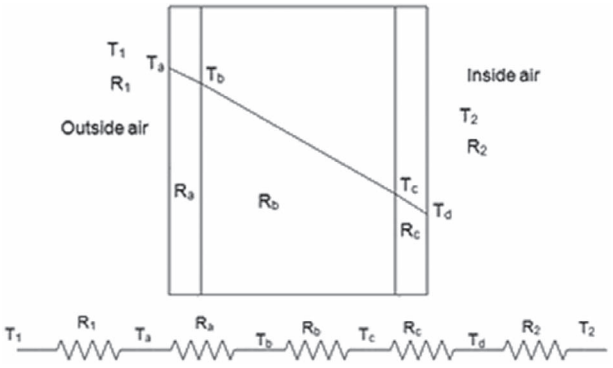

Figure 8. Thermal model and resistance diagram of conventional wall.

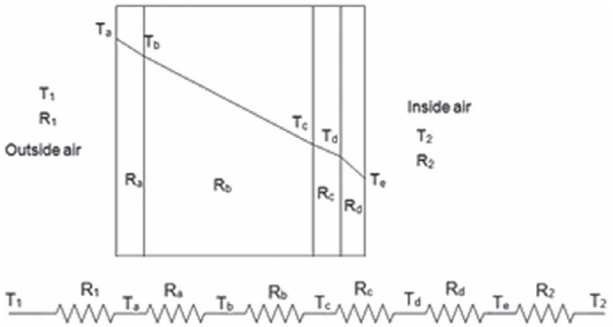

Figure 9. Thermal model and resistance diagram of insulated wall.

2.4 Life-cycle cost analysis

LCCA is a method of calculating the total cost of equipment including initial cost, operating cost, and disposing cost. This analysis is carried out to compare the cost of alternatives with that of current equipment to increase the savings. The basic formula for calculating the life cycle cost is as follows:

$$\text{LCC} = \text{Initialcost} + \text{Recurringcost} - \text{Residualcost} \quad (14)$$

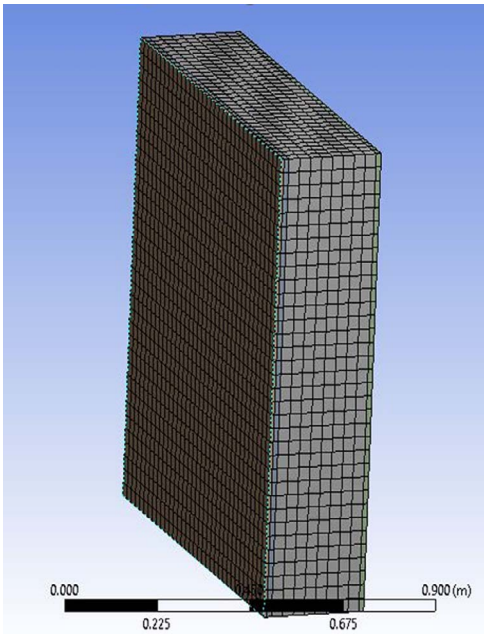

Figure 10. Meshed geometry of wall.

Use of HVLS fan is an active cooling technique, and aluminium bubble wrap insulation is a passive cooling technique for improving thermal comfort inside a building. The life-cycle cost involved around the implementation of these techniques was studied and compared in this section. Initial cost is the cost involved in procuring and installation. Recurring costs are the cost involved after installation such as operation cost, maintenance cost, etc. Finally, the residual cost is value of the product after its life span. For this project, the life-cycle costs of HVLS fan and aluminium bubble wrap are calculated and compared to know the best solution to thermal comfort inside

Table 6. Film coefficient and ambient temperature of air.

	Film coefficient (Wm^{-1} K^{-1})	Ambient temperature (°C)
Outside	23	37
Inside	9	25

Figure 11. HVLS fan.

the workshop complex. Nowadays, HVLS fans are used in industrial buildings and workshops for the thermal comfort inside the buildings. The HVLS fan installed in the workshop where this study is carried out is MG245 model and it is shown in Fig. 11. The fan diameter and power are 24 feet and 1.5 kW, respectively.

Initial cost of the HVLS fan is 1,94 700 INR. Electrical energy consumed per day by the HVLS fan is calculated below:

$$E = P \times t \tag{15}$$

where E is the electrical energy in kWh, P is the power in kW, and t is the time in hours per day. For 6 hours of operation, the electrical energy consumed is calculated as 9 kWh.

Price of one unit current is 7.5 INR for private institutions [42]; therefore, the cost for electricity per year is 24 637 INR. Residual cost is assumed to be 20 000 INR. The aluminium bubble wrap which is shown in Fig. 12 is a double layer of 4 mm thick bubble sheet laminated on both sides with pure aluminium foil, or a combination of pure aluminium foil and metalized film, poly film, or woven aluminium film. Use of aluminium foil is a cost effective passive technique for reducing the heat radiation. Heat penetration into the room from the walls is reduced using the aluminium bubble wrap. The novelty of this study is that the material which is used as insulation material for roof is used to reduce the heat transfer from wall to the room. This type of passive technique has not been studied for gable roofed working area which is also as a novelty.

$$\text{Initial cost} = \text{Total area} \times \text{Cost per unit area} \tag{16}$$

Cost per square feet of 8 mm sheet is 16 INR.

Total area as per Table 7 is 9185.7 square feet. By Equation (16), the initial cost is estimated as 146971.36 INR.

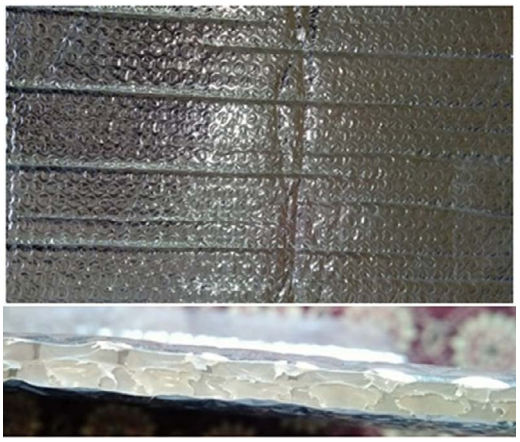

Figure 12. Aluminium bubble wrap.

Table 7. Area of walls.

Wall	Area (m^2)
Wall 1 (North side)	102.81
Wall 2 (West side)	52.95
Wall 3 (South side)	141.6
Wall 4 (East side)	141.6
Roof	414.42
Total area	853.38

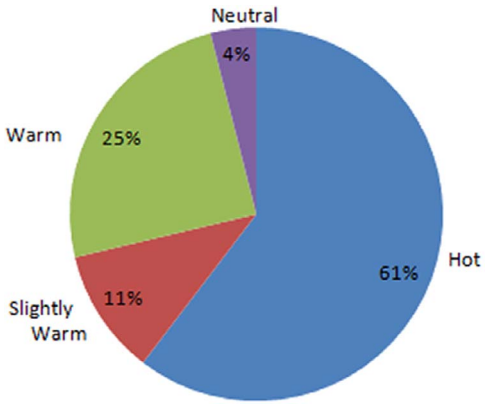

Figure 13. Survey results about thermal sensation inside the workshop.

There is no operating and residual costs in aluminium bubble wrap insulated walls. 200°C is the melting temperature of aluminium bubble wrap, and it can catch fire at 500°C. Bubble wrap made of aluminium is a safe material to use as insulation because of these two characteristics.

3 Results and discussions

From the questionnaire responses, it was observed that 61% of the inmates experienced high thermal discomfort. Approximately 59% of the persons reported that the time of discomfort was between 2 pm and 5 pm and 32% reported that there was always a thermal discomfort inside the working area. The thermal sensation of the people in the workshop is depicted in Fig. 13 in the form of pie chart. The survey was conducted during the month of March which is a summer season in India. The mean ambient temperature outside the

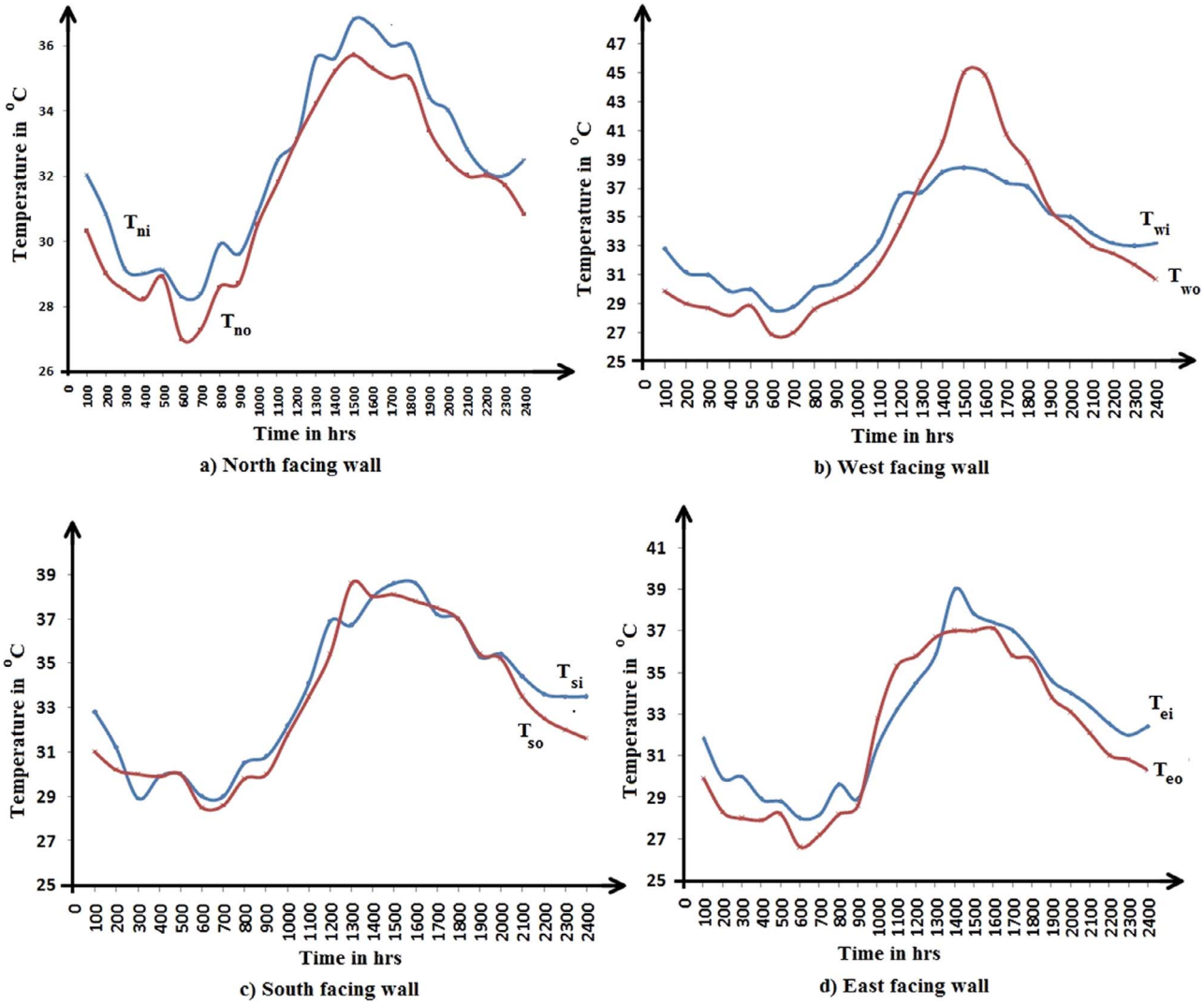

Figure 14. Temperature profile at the inner and outer surface of the wall.

shed varied between 38°C and 40°C, and the relative humidity varied between 55% and 65%.

Also, the increase in wall and floor temperatures causes discomfort according to the direction of heat flow. The inside air temperature had its peak value of 36.5°C at 3.00 pm, and the outside air temperature reached the peak at 2.00 pm. The air temperature inside the workshop, inside the staff cabin, and outside the workshop varies in a sinusoidal manner. The solar radiation enters the building envelope through the different modes of heat transfer. A portion of the indoor air absorbs the penetrated heat while most of the radiation heat from the sun is absorbed by the walls and roof. Due to the large but finite thermal capacity of the roof, floor, and walls, their temperature increase slowly due to the absorption of radiant heat. The radiant portion introduces a time lag and also a decrement factor depending upon the dynamic characteristics of the surfaces. Due to the time lag, the effect of radiation will be felt even after the elimination of the radiation source. Also, the convective heat transfer on the outer surface of the wall is not equal to that of the inside surface of the wall. The evaluation of heat transfer by drawing thermal resistance diagrams will be of no use if the heat transfer is not steady. Figure 14 shows the variation of inner and outer surface temperatures of the four walls during a time period of 24 hours. In the north facing wall, the inside surface temperature was always greater than the outside temperature. For the west facing wall, the temperature differences between the inner and outer surface are significantly higher as the wall is exposed to direct solar radiation in the afternoon. The conduction heat transfer across the walls starts from inner to outer surface in almost all the cases. When compared with the outer surface temperature, the inside surface temperature was higher from 1.00 pm to 7.00 pm in the case of west facing wall, 10.00 am to 11.00 am in the case of south facing wall and 10.00 am to 1.00 pm in the case of east facing wall. From midnight to 10.00 am, the temperature of external air is lower than that of indoor air. After that, the external air temperature increases and remains higher compared to that of the indoor air. The average temperature inside the cabin was higher than the average indoor air temperature. From the mathematical models, the temperature of the walls at every 6 mm from the origin in x direction is captured and plotted in the graph. This is repeated for four walls corresponding to the temperature reading of 3.00 pm as it is considered as a steady state.

From Fig. 15, it was clearly understood that the nature of heat transfer in wall 2 differs from all other walls. Across wall

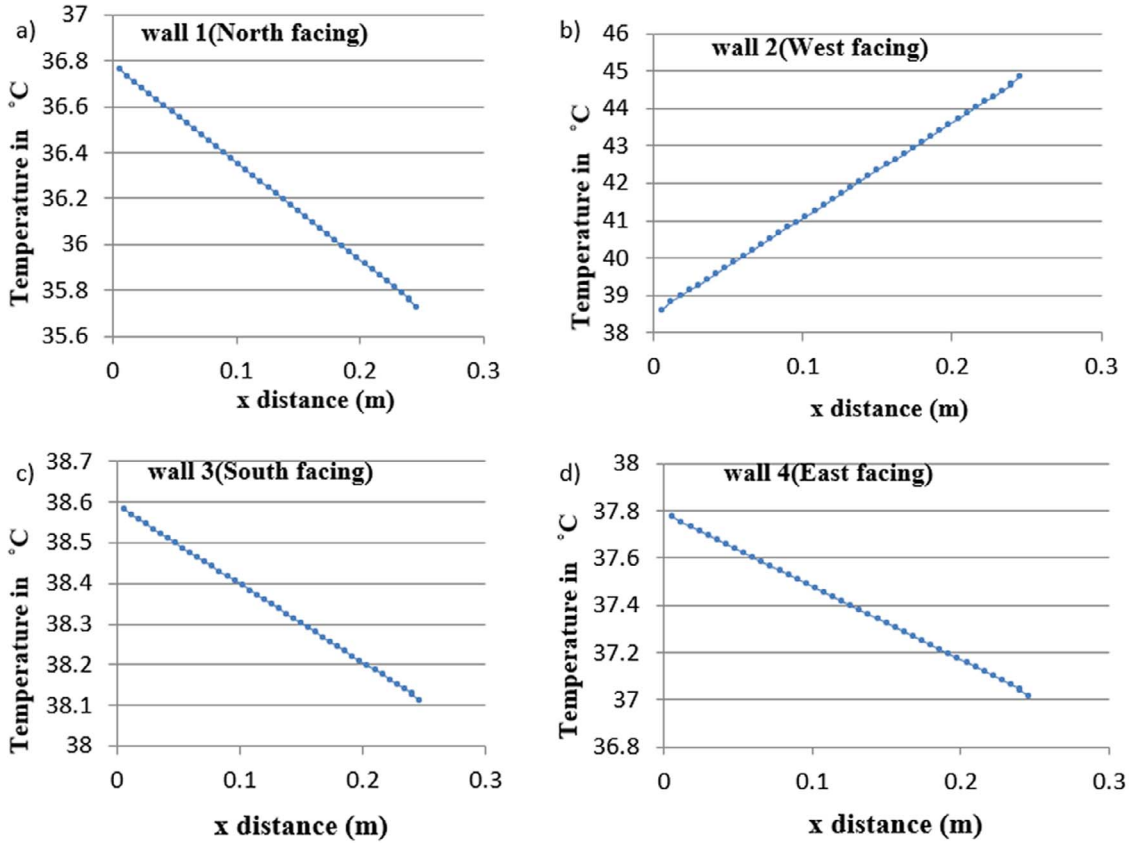

Figure 15. Temperature at every 6 mm in the wall.

2 heat flows from outside the building to the room whereas in all other walls, it is inversed. The main reason behind the phenomenon in wall 2 alone is the location of the workshop complex. As shown in Fig. 4, wall 2 faces the west direction and the chosen time is 3.00 pm when the sun's radiation is comparatively higher than any time.

From Fig. 16, it can be seen that except the west facing wall, all the walls are covered by other buildings. At the time of 3.00 PM, the sun is on the western side and heating the west facing wall directly. The temperature of the wall is not a constant value because of time lag. Thicker material takes longer time for heat waves to pass through, and therefore, the maximum temperature at 3.00 PM is not due to the instant heat radiation. It is the temperature raised because of the heat penetrated from the morning hours. The ANSYS simulations for the one-dimensional heat conduction across the four walls are shown in Fig. 17.

From the simulation results of the four walls, the intermediate temperature of each wall is noted. These temperatures are compared with the intermediate temperatures calculated from the Equations (4) and (5) and presented in Table 8.

The maximum percentage deviation of numerical simulation result from the mathematical model is identified for west facing wall. The temperature difference between the outer and inner surfaces of the west facing wall is significantly higher. This is because of increased convective heat transfer between wall and surrounding air. The numerical results give accurate results when the governing equations are solved with exact boundary conditions. In total, the overall deviation between numerical and mathematical model is less than 0.2% which makes the model fit enough for repeated analysis. Figures 18 and 19 show the temperature distribution inside the workshop which is obtained from ANSYS simulation. In Fig. 18, the highest temperature inside the workshop is seen at the roof area. From the roof at 325 K, maximum heat was gained by the air inside the workshop complex and a minimum temperature of 310.8 K was recorded. The air temperature obtained from the simulation result is compared with the actual air temperature measured inside the workshop complex at 3.00 PM and the difference in the value is 2.5°C. The natural conventional heat transfer inside the rectangular enclosure (bottom section without roof) causes density changes in air layer and makes the air to move in particular direction. Figure 20 shows the velocity vector of air inside the workshop

Figure 16. Satellite image of workshop complex.

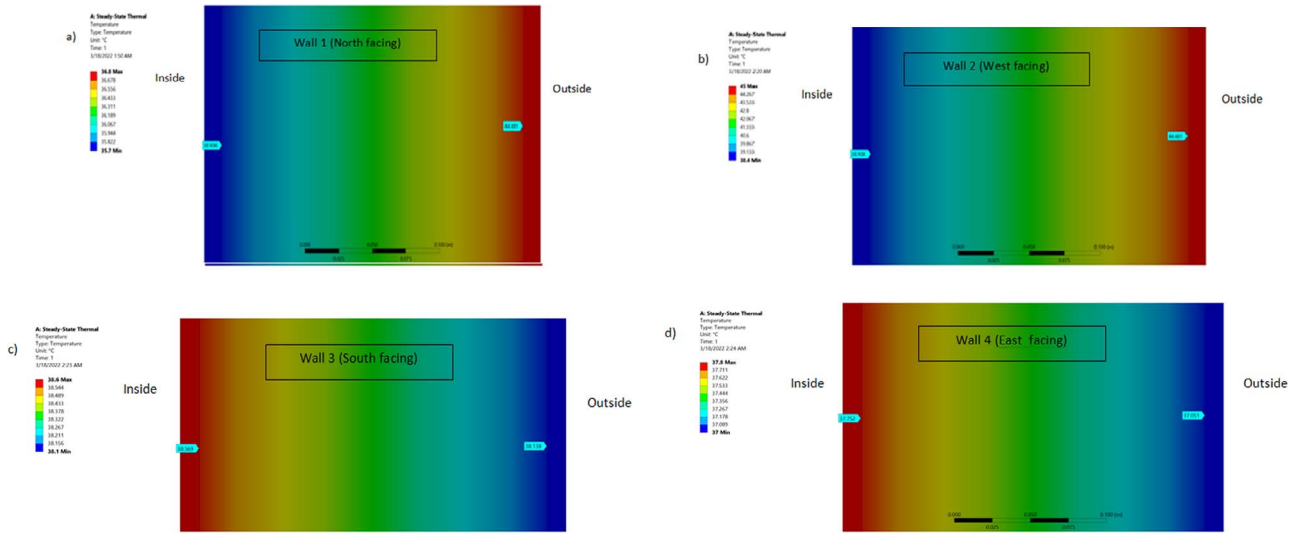

Figure 17. Simulation results of 1D heat conduction (a) North facing wall (b) West facing wall (c)South facing wall (d)East facing wall.

Table 8. Comparison of results from numerical and mathematical models.

	Intermediate temperature (T_b) (°C)			Intermediate temperature (T_c) (°C)		
	Mathematical model	Numerical simulation	% deviation	Mathematical model	Numerical simulation	% deviation
North facing wall	36.73	36.73	0.00	35.77	35.78	0.03
West facing wall	38.83	38.90	0.18	44.48	44.56	0.18
South facing wall	38.56	38.56	0.00	38.13	38.14	0.03
East facing wall	37.74	37.75	0.03	37.05	37.05	0.00

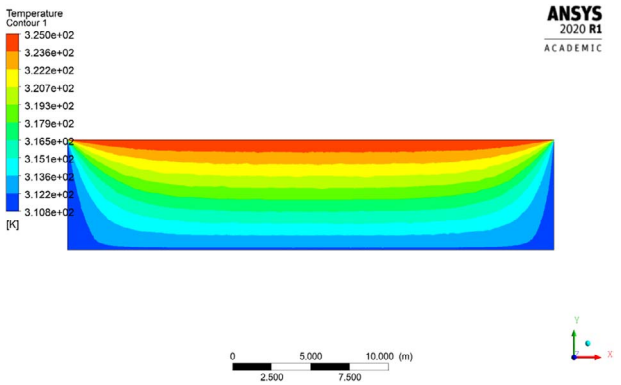

Figure 18. Simulation result of convection heat transfer of section A–A of workshop complex.

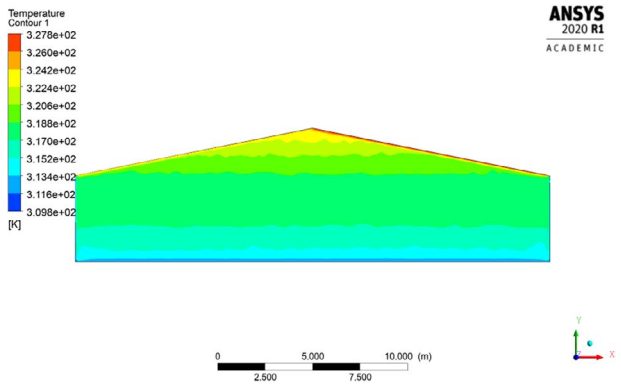

Figure 19. Simulation result of convection heat transfer of section B–B of workshop complex.

complex. The buoyancy effect of air is resulted because of the high temperatures prevailing near the walls and roof surfaces. Uniform movement of air is seen only near to the walls.

There are many active and passive cooling systems available for reducing the indoor temperature. The feasible solutions that do not involve alterations in the building structures are only considered for this study. The internal heat gain can be reduced by using rooftop solar PV panels, false ceiling, or high volume low speed fan. The latitude and longitude of the location is 11.27°N and 77.60°E. The total roof area available for rooftop solar panels is 791 m^2. The commercial panel size available in the market is 1 m × 2 m with rating of 325 Watts. A total of 280 panels can be installed over the metallic roofing, and this will be capable of producing 91 kW electric power. The design of a PV system involves the selection of battery, inverter, and PV panels. The approximate cost of the 91 kW solar PV system is 75 lakh INR. For providing false ceiling, the floor area is calculated and based on it the total cost of false ceiling is estimated as 8.5 lakhs INR(100 INR/sq.ft). The airflow for ventilation depends on area in the area method, volume of space in air change method, number of occupants in occupancy method, and heat to be removed in the heat removal method. Since the warehouse is volume dominant, the air change method would be the best option for estimating air flow. The ACH for the workshop is assumed to be 12. With 155631.7 m^3 of volume, the air flow in CFM is calculated as 31126.3 using Equation (17).

$$\text{Air flow in CFM} = \text{Volume} \times \frac{\text{ACH}}{60} \tag{17}$$

Table 9. Comparison of mathematical and numerical result of heat flux.

Wall type	Heat flux from mathematical model (Wm^{-2})	Heat flux from numerical model (Wm^{-2})	Percentage deviation
Non-insulated wall	28.67	28.63	0.14
Insulated wall	20.65	19.05	7.74

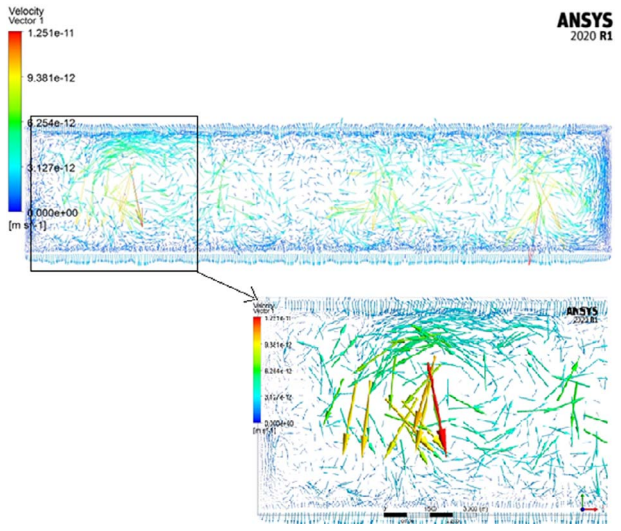

Figure 20. Simulation of velocity vectors inside the workshop complex.

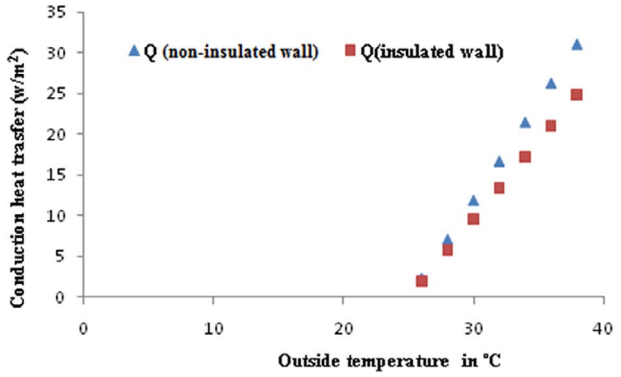

Figure 21. Effect of insulation on conduction heat transfer.

A HVLS fan which can deliver the above quantity of air costs 2 Lakhs INR approximately. The passive cooling technique of insulating the wall is compared with the active cooling technique. The *U* value for the wall without insulation was calculated as 2.387 W/m^2K using Equation (14), and it was found to be within the maximum *U* value limited by the bureau of Indian standards given in Table 5. The heat conduction (Q) from outside to inside across the non-insulated wall is calculated as 31.036 W using Equation (15). For the wall insulated with a 4 mm aluminium bubble wrap, the *U* value and conduction heat transfer (Q) were found to be 1.907 W/m^2K and 24.803 W, respectively. The graph comparing the conduction heat transfer across noninsulated and insulated walls for varying outside temperatures is plotted in Fig. 21.

The maximum heat fluxes interpreted from the numerical simulation of noninsulated and insulated walls are 28.63 Wm^{-2} and 19.05 Wm^{-2}. The simulation results are compared with the mathematically solved solutions from Equation (15) in Table 9.

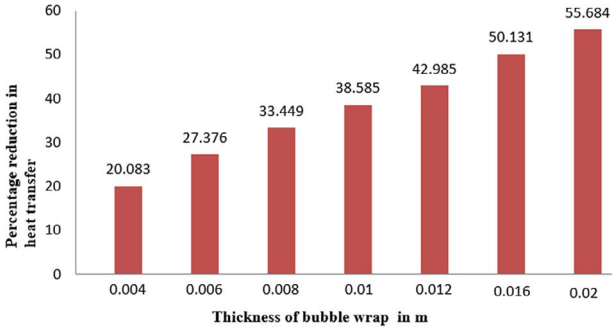

Figure 22. Percentage reduction of heat transfer inside workshop.

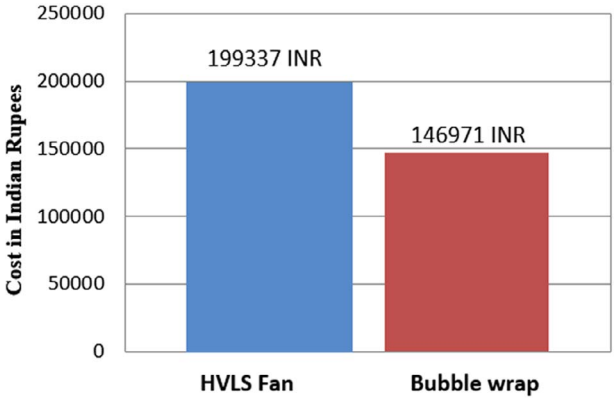

Figure 23. LCCA of HVLS fan and aluminium bubble wrap.

Thickness of the aluminium bubble wrap can be increased to reduce the convection heat to the inside air. Figure 22 shows the percentage reduction in heat transfer inside the workshop complex due to varying thickness of aluminium bubble wrap.

The percentage reduction in heat transfer due to aluminium bubble wrap insulation is calculated Equation (18).

$$\%\text{improvement} = \left(\frac{Q_{\text{wall without insulation}} - Q_{\text{wall with insulation}}}{Q_{\text{wall without insulation}}}\right) \times 100 \quad (18)$$

At least 20.08% of heat transfer can be reduced by using a 4-mm thick aluminium bubble wrap for insulation. The maximum possible heat reduction of 55.68% can be achieved with a 20-mm thick insulation. The choice of selecting an appropriate passive building cooling technique depends the institution's potential to invest money in the project. The project cost for employing the aluminium bubble wrap insulation is expected to be 8–10 lakhs INR for the selected workshop area. In order to reduce the cost, viable alternatives are studied and the idea of using HVLS fan which is an active cooling method is considered for this work.

The graph comparing the life cycle cost of HVLS fan and aluminium bubbles wrap insulation is shown in Fig. 23. The cost required for providing aluminium bubble wrap is 146971.36 INR which is calculated according to the area 9185.7 square feet shown in Table 7.

In order to reduce the heat by 33% inside the workshop, HVLS fan of worth 2 lakhs INR or 8 mm thick aluminium bubble wrap insulation of worth 1.5 lakhs INR may be used. When two alternatives are available for mitigating a problem, the selection of technology will purely depend on the cost factor. The operating cost in the case of HVLS fan is a critical factor. If solar power is used for running HVLS fan, the cost of solar photovoltaic plant, the return on investment, and plant maintenance cost are to be considered carefully. But in the case of aluminium bubble wrap, no hidden costs are found. The life of aluminium bubble wrap is between 5 and 7 years, and this seems to be a best passive cooling technology for education institutions having gable-roofed metallic shed. From the above discussions, it was justified that insulating the workshop with 8 mm thick aluminium bubble wrap will be a cost effective method to ensure thermal comfort inside the building.

4 Conclusion

Thermal comfort inside a gable roof shed was studied independently with HVLS fan and aluminium bubble wrap insulation. Questionnaire method was used to gather data from the participants about thermal comfort. Temperature measurements showed high temperatures prevailing within the workshop. Significant results from the study were reported below:

- Thermal discomfort in gable roofed workshops were highly reported during 2 PM to 5 PM.
- By implementing a passive cooling technique such as wall and roof insulation, the percentage reduction of conduction heat transfer varies from 20.08% to 55.68% when using various thickness of aluminium bubble wrap.
- From LCCA between aluminium bubble wrap and HVLS fan, bubble wrap found to be the economical passive cooling technique that improves thermal comfort.. The computer simulated results deviate only by less than 0.1% in comparison to the theoretical model.
- For the insulated wall, the U value and conduction heat transfer (Q) for the 4 mm aluminium bubble wrap was found to be 1.907 W/m^{2}K and 24.803 W respectively.
- Solar heat gain removal inside the room using roof top solar photovoltaic plant is not economical as it involves more than 50 lakhs INR.

For the future work, the implementation of insulating material in the workshop and analyzing the real-time thermal comfort inside the workshop complex can be carried out. The evaluation of thermal comfort helps in moving towards a better indoor environment.

Declaration of Competing Interest

The authors declare that they have no known competing financial interests or personal relationships that could have appeared to influence the work reported in this paper.

Funding

None declared.

References

1. Das B, Dutta PP, Bardalai M. *et al.* Comparative study on performance of high volume low speed (HVLS) fans with high-speed fans for the use in dairy barns. *Mater Today Proc* 2021;**47**:4606–10.
2. Macher, Boudhaim M, Grussenmeyer P. *et al.* Combination of thermal and geometric information for BIM enrichment. *Int Arch Photogramm Remote Sens Spat Inf Sci* 2019;**42**:719–25.
3. Zhao P, Zhu N, Chong D. *et al.* Developing a new heat strain evaluation index to classify and predict human thermal risk in hot and humid environments. *Sustain Cities Soc* 2022;**76**:103440.
4. Abd Rahman NM, Haw LC, Fazlizan A. *et al.* Thermal comfort assessment of naturally ventilated public hospital wards in the tropics. *Build Environ* 2022;**207**:108480.
5. Mirzabeigi S, Nasr BK, Mainini AG. *et al.* Tailored WBGT as a heat stress index to assess the direct solar radiation effect on indoor thermal comfort. *Energy Build* 2021;**242**:110974.
6. González J, Soares CAP, Najjar M. *et al.* BIM and BEM methodologies integration in energy-efficient buildings using experimental design. *Buildings* 2021;**11**:491.
7. de Melo Pinto N, de Paula Xavier AA, Hatakeyama K. Thermal comfort in industrial environment: conditions and parameters. *Procedia Manuf* 2015;**3**:4999–5006.
8. Jing S, Lei Y, Wang H. *et al.* Thermal comfort and energy-saving potential in university classrooms during the heating season. *Energy Build* 2019;**202**:109390.
9. Kusuda T. Fundamentals of building heat transfer. *J Res Natl Bur Stand* 1977;**82**:97–106. https://doi.org/10.6028/jres.082.008.
10. Elaouzy Y, El Fadar A. A multi-level evaluation of bioclimatic design in Mediterranean climates. *Sustain Energy Technol Assessments* 2022;**52**:102124.
11. Hussain A, Blanchet P. Preparation of breathable cellulose based polymeric membranes with enhanced water resistance for the building industry. *Materials* 2021;**14**:4310.
12. Ali MF, Natarajan MMV. Thermal insulation of building envelope for ecological conservation. In: Malik JA, Marathe S (eds.), *Ecological and Health Effects of Building Materials*. Cham: Springer, 2022. https://doi.org/10.1007/978-3-030-76073-1_11
13. Maduru VR, Shaik S, Cuce E. *et al.* Analysis of effective parameters of building's glazing on energy savings and carbon emission mitigation prospective. *Int J Ambient Energy* 2022;**43**:8959-70. https://doi.org/10.1080/01430750.2022.2111348.
14. Huelsz G, Barrios G, Rojas J. Differences on results from steady-state and time-dependent wall/roof heat transfer models in Mexican climates. *Energy Procedia* 2014;**57**:1825–33.
15. Al-Sanea SA. Evaluation of heat transfer characteristics of building wall elements. *J King Saud Univ-Eng Sci* 2000;**12**:285–312.
16. Cheng X, Zou Z, Yu G. *et al.* Development and performance of roof-based building-integrated photovoltaic-thermal systems: a review. *J Sol Energy Eng* 2021;**143**:041009.
17. Amrani A, Dihmani N, Amraqui S. *et al.* Analysis of combined natural convection and thermal radiation heat transfer in a triangular shaped roof for hot climates. *J Mater Environ Sci* 2017;**8**:3013–27.
18. Yıldırım Evd. Investigation of the effect of the roof geometry on building thermal behaviour. *Uludağ Universitesi Muhendislik Fakultesi Dergisi* 2017;**22**:187–200.
19. Vanaga R, Blumberga A, Purvins R. *et al.* Heat transfer analysis by use of lense integrated in building wall. *Energy Procedia* 2017;**128**:453–60.
20. Family R, Mengüç MP. Materials for radiative cooling: a review. *Procedia Environ Sci* 2017;**38**:752–9.
21. Pisello AL, Castaldo VL, Piselli C. *et al.* Combined thermal effect of cool roof and cool façade on a prototype building. *Energy Procedia* 2015;**78**:1556–61.
22. Nugroho AM. Vertical landscape for passive cooling in tropical house. *Procedia Environ Sci* 2014;**20**:141–5.
23. Sudprasert S, Sankaewthong S. Utilization of rice husks in a water-permeable material for passive evaporative cooling. *Case Stud Constr Mater* 2018;**8**:51–60.

24. Dehghani-sanij AR, Soltani M, Raahemifar K. A new design of wind tower for passive ventilation in buildings to reduce energy consumption in windy regions. *Renew Sust Energ Rev* 2015;**42**: 182–95.
25. Pandiaraj S, Jaffar AA, Muthusamy S. *et al.* A study of solar heat gain variation in building applied photovoltaic buildings and its impact on environment and indoor air quality. *Energy Sources A: Recovery Util Environ Eff* 2022;**44**: 6192–212.
26. Charney W (ed). *Handbook of Modern Hospital Safety*, 2nd edn. CRC Press, 2009. https://doi.org/10.1201/9781420047868.
27. Hassan SA. The role of cooling degree days on determining the insulation of building envelop in a hot climate (Iraqi cities as an example). In: *IOP Conference Series: Materials Science and Engineering*, vol. **584**. IOP Publishing, 2019, 012009.
28. Zhu Y, Wang X. Thermal insulation performance of radiant barrier roofs for rural buildings in the qinba mountains. *Math Probl Eng* 2020;**2020**:1–13.
29. Loggia R, Flamini A, Massaccesi A. *et al.* A case study of a renovation of a historical university department: the nearly zero-energy refurbished buildings. *IEEE Trans Ind Appl* 2022;**58**: 6970–80.
30. Maruf Ahmed SM, Masum Ahmed SM, Zeyad M. An approach of a Nearly Zero-Energy Building (nZEB) to build an official zone with Micro-grid. In: *2020 6th IEEE International Energy Conference (ENERGYCon)*, Gammarth, Tunisia, 2020, 662–7. https://doi.org/10.1109/ENERGYCon48941.2020.9236548.
31. Ismaila MA, Rashid FA. Green architecture approach toward sustainable mosques in Malaysia. *Jurnal Kejuruteraan* 2023;**35**: 693–8.
32. Alhasan O, Lobanov K. *Transforming Warehouses Towards a Sustainable Future. Massachusetts Institute of Technology, USA,* 2023.
33. Lu K, Deng X, Jiang X. *et al.* A review on life cycle cost analysis of buildings based on building information modeling. *J Civ Eng Manag* 2023;**29**:268–88.
34. Howell KB. *Principles of Fourier analysis*. CRC Press, Boca Raton 2016.
35. Jayamaha S, Wijeysundera N, Chou S. Measurement of the heat transfer coefficient for walls. *Build Environ* 1996;**31**:399–407.
36. Kothandaraman C. *Heat and mass transfer data book*. New Age International, New Delhi 2004.
37. Sachdeva R. *Fundamentals of Engineering Heat and Mass Transfer*. New Age International, New Delhi 2006.
38. Mohammadi F, Shontz SM. A direct method of generating quadratic curvilinear tetrahedral meshes using an advancing front approach. *Proceedings of the 29th International Meshing Roundtable*, National Science Foundation, Virginia 2021.
39. Wang W, Chen Z, Zhang X. *et al.* Study on fabrication and properties of the aluminum foil/bubble composite. *ICCM Int Conf Compos Mater* 2017;20–25.
40. Khabaz A. Construction and design requirements of green buildings' roofs in Saudi Arabia depending on thermal conductivity principle. *Constr Build Mater* 2018;**186**:1119–31.
41. Kishore KN, Rekha J. A bioclimatic approach to develop spatial zoning maps for comfort, passive heating and cooling strategies within a composite zone of India. *Build Environ* 2018;**128**: 190–215.
42. Lavanya A, Divya Navamani J, Geetha A. *et al.* Smart energy monitoring and power quality performance based evaluation of 100-kW grid tied PV system. *Heliyon* 2023;**9**:e17274.